Cycle-Slip Detection Using Soft-Output Information

Xiaowei Jin, Aleksandar Kavčić
Division of Engineering and Applied Sciences
Harvard University, Cambridge, MA 02138
Email: {xjin, kavcic}@hrl.harvard.edu

Abstract-To realize their full coding gain potential, iterative decoders need to operate in low signal-to-noise ratio (SNR) regions where timing recovery devices experience cycle-slips. This paper develops a binary Bayesian cycle-slip detector by using soft-output information. A practical decision rule is derived utilizing a series of approximations. Approximate analytic expressions for the probabilities of cycle-slip detection and false alarm are obtained. They guide us in choosing detector parameters that will meet a desired performance specification. The applicability of this method is shown on artificially generated waveforms.

I. INTRODUCTION

In recent years, iterative decoders of turbo codes [1] and low-density parity check (LDPC) codes (Gallager codes) [2] have shown performance approaching the Shannon limit for additive white Gaussian noise channels [3]–[6]. Iterative decoding has also been proposed for partial response channels showing comparable coding gains [7]–[11].

Since iterative decoders can operate at very low SNRs, they must rely on timing recovery devices (synchronizers) that are capable of tracking the phase error at these same SNRs. In magnetic recording, most synchronizers are decision-directed hybrid error-tracking devices (e.g., the Mueller and Müller synchronizer [12]). At low SNRs, these synchronizers fail due to cycle-slips. This is illustrated in Fig. 1, where on an ideal Nyquist band-limited channel with no intersymbol interference (ISI), the performance of MacKay's rate 4/5 code [13] is shown for an ideal synchronizer (using perfect timing information), and for a Mueller and Müller (M&M) synchronizer. While the system with the ideal timing information reaches error rates of 10^{-4} at SNR [1] of 5.15 dB, the system with a realistic synchronizer is, due to cycle-slips, incapable of operating at SNRs below 6.5dB, which is the region of interest.

Since iterative decoders typically provide preliminary soft decisions after every iteration, it makes sense to use these soft decisions to iteratively fine-tune the timing estimates (e.g., using the EM algorithm [14]). However, the initial timing estimates need to be good in order to have convergence for the iterative synchronizers. An important task is to eliminate the cycle-slips. This paper deals with the problem of detecting cycle-slips. The channel model chosen for this paper is the ISI-free binary band-limited channel, but the method developed in this paper can be applied to a general ISI channel if the soft output information is properly extracted. In Section II we introduce the cycle-slip problem in synchronizers. Section III formulates the Bayesian cycle-slip detection problem. We introduce in Section IV several approximations to simplify the decision rule. In Section V the decision rule is applied to generated waveforms. Section VI concludes the paper.

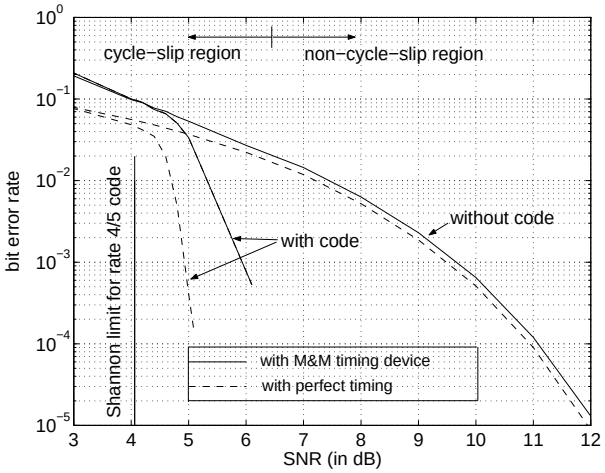

Fig. 1. Error rate comparison between a system with ideal timing recovery and Mueller and Müller (M&M) timing recovery.

Notation: Throughout the paper, the acronym "i.i.d." stands for "independent identically distributed", $x \sim \mathcal{N}\left(m, \sigma^2\right)$ denotes that the random variable x is normally distributed with mean m and variance σ^2, and "pdf" stands for probability density function. The superscript ^{T} is used to denote vector transposition. $E\left[x\right]$ and $\mathrm{Var}\left[x\right]$ stand for the mean and variance of the random variable x, respectively.

II. CYCLE-SLIPS IN SYNCHRONIZERS

Let $\{a_m\}$ denote a sequence of equally probable i.i.d. symbols that take values from $\{-1, 1\}$. The baseband pulse amplitude modulated (PAM) pulse is denoted by $h\left(t\right)$. The received noisy PAM signal is given by

This work was supported in part by NSF under Grant CCR-9984297 and by IBM Corporation.

[1] SNR is defined as $10\log_{10}\frac{\mathrm{P}}{\sigma^2}$, where σ^2 is the variance of the noise, and P is the power of the signal, here we assume P=1.

$$z(t) = \sum_{m=-\infty}^{\infty} a_m h(t - mT - \varepsilon_m T) + n(t). \qquad (1)$$

where $n(t)$ is zero mean white Gaussian noise, and $\varepsilon_m = \varepsilon(mT)$, where $\varepsilon(t)$ is a *slowly* varying phase drift. We assume that $h(t)$ is strictly band-limited and $h(t) = \text{sinc}\left(\frac{t}{T}\right) = \frac{\sin(\pi t/T)}{\pi t/T}$. The signal in (1) is matched-filtered and sampled at time instants $kT + \hat{\varepsilon}_k T$ to produce an output sample

$$z_k = \sum_{m=-\infty}^{\infty} (a_m + n_m) \,\text{sinc}\left[k - m - (\hat{\varepsilon}_k - \varepsilon_m)\right], \qquad (2)$$

where $\hat{\varepsilon}_k$ is the estimate of ε_k, and n_m is i.i.d. with distribution $\mathcal{N}\left(0, \sigma^2\right)$.

In order to correctly detect the symbol sequence, the receiver needs a timing recovery device to estimate the unknown normalized phase delay $\hat{\varepsilon}_k$ at the k-th sample point. Typically, the synchronizer is suitably chosen to minimize a penalty function (usually the variance) of the timing error $\epsilon_k = \hat{\varepsilon}_k - \varepsilon_k$. Since the received waveform $z(t)$ is cyclostationary with period T [15], there is no difference in the signal statistics if the normalized phase delay is $\varepsilon(t)$ or $\varepsilon(t) + m$, where $m \in \mathbb{Z}$. Thus, the synchronizer has many stable operating points. Most of the time, the estimated value $\hat{\varepsilon}_k$ tracks the true phase delay ε_k with small random fluctuations. The value of $|\epsilon_k|$ is close to zero around these points. If the estimate deviates too far away from the true value, it will go into a neighboring stable operating point and keep tracking the new normalized phase with a ± 1 difference. This is called a cycle-slip. In the cycle-slip region, the value of $|\epsilon_k|$ is close to $\frac{1}{2}$. The synchronizer will stay at the new stable point until the next cycle-slip occurs. At low SNRs, cycle-slips are more likely to occur, which always results in a burst of symbol errors and thus a burst of decoding errors.

We define a confidence region where we can consider that there is no cycle-slip, as a region on the time axis k for which

$$|\epsilon_k| = |\hat{\varepsilon}_k - \varepsilon_k| \leq \epsilon^{(0)}, \qquad (3)$$

where $\epsilon^{(0)}$ is chosen to reflect the statistics of the timing recovery device we are using ($\epsilon^{(0)}$ should be a number close to 0, we assume $\epsilon^{(0)} \leq \frac{1}{4}$ in the sequal). Similarly, we define a confidence region where we consider that a cycle-slip is occurring, as a region on the time axis k for which

$$\left|\frac{1}{2} - |\epsilon_k|\right| \leq \left|\frac{1}{2} - \epsilon^{(1)}\right| \quad , \qquad (4)$$

where $\epsilon^{(1)}$ is chosen to reflect the statistics of the synchronizer ($\epsilon^{(1)}$ should be a number close to $\frac{1}{2}$). If we choose $\epsilon^{(1)}$ to be $\frac{1}{2}$, then (4) defines the exact middle point between the attraction domains of two neighboring stable operating regions. Our task is to distinguish between a cycle-slip and a non-cycle-slip, i.e., whether (3) or (4) is a better hypothesis. Since both (3) and (4) define a continuous region in ϵ, we can make the test more conservative by testing only at the boundaries of these regions. This is the motivation for the binary Bayesian cycle-slip detection problem presented in Section IV. Since both ε_k and $\hat{\varepsilon}_k$ are slowly time-varying, the value ϵ_k also stays constant over several symbol intervals (even during a cycle-slip). We use this to motivate our "time-invariance" assumption in Section III.

III. Bayesian detection of cycle-slips using soft-output information

Let us assume that both $\varepsilon_k = \varepsilon$ and $\hat{\varepsilon}_k = \hat{\varepsilon}$ are time invariant. Let us also assume that their absolute difference $|\epsilon| = |\hat{\varepsilon} - \varepsilon|$ can take only two values: $\epsilon^{(0)}$ or $\epsilon^{(1)}$. We then define the following two hypotheses

$$\begin{aligned} H_0 &: |\epsilon| = \epsilon^{(0)} &&\Longrightarrow \text{no cycle–slip} \\ H_1 &: |\epsilon| = \epsilon^{(1)} = \frac{1}{2} &&\Longrightarrow \text{cycle–slip} \quad . \end{aligned}$$

We assume that at time k the detector computes the soft-output μ_k (log-likelihood ratio of two output-value pdfs evaluated at the obtained sample value) using the best guess that it has perfect synchronization ($\epsilon = 0$). In our case, since we are assuming i.i.d. equally likely symbols [1],

$$\mu_k = \ln\left[\frac{p(z_k|\epsilon = 0, a_k = 1)}{p(z_k|\epsilon = 0, a_k = -1)}\right] = \frac{2z_k}{\sigma^2}. \qquad (5)$$

Assume a window of W observations μ_k $(k = 1, \cdots, W)$ is available.

Under hypothesis H_i (assuming $\epsilon^{(i)} > 0$)[2],

$$\begin{aligned} \mu_k &= \frac{2z_k}{\sigma^2} = \frac{2}{\sigma^2}\sum_m (a_{k-m} + n_{k-m}) \text{sinc}\left(m - \epsilon^{(i)}\right) \\ &= \frac{2}{\sigma^2}\sum_m a_{k-m} \text{sinc}\left(m - \epsilon^{(i)}\right) + \nu_k, \qquad (6) \end{aligned}$$

where $i \in \{0, 1\}$, and $\nu_k = \frac{2}{\sigma^2}\sum_m n_{k-m} \text{sinc}\left(m - \epsilon^{(i)}\right)$ is i.i.d. $\mathcal{N}\left(0, \frac{4}{\sigma^2}\right)$ by the sampling theorem for band-limited Gaussian random processes [16]. Denoting by $p\left(\underline{\mu}_1^W | H_i\right)$ the *joint* pdf of $\underline{\mu}_1^W = [\mu_1, \cdots, \mu_W]^{\mathrm{T}}$ under hypothesis H_i, the likelihood ratio test is

$$\frac{p\left(\underline{\mu}_1^W | H_0\right)}{p\left(\underline{\mu}_1^W | H_1\right)} \underset{H_1}{\overset{H_0}{\gtrless}} \eta, \qquad (7)$$

[1] Even though μ_k is proportional to the observation z_k, we use μ_k throughout this paper in anticipation of applying a similar method to ISI channels where the density of μ_k stays bimodal, but the density of z_k is no longer bimodal.

[2] Since the statistics of μ_k are the same for $\epsilon^{(i)} < 0$, we only consider the case $\epsilon^{(i)} > 0$.

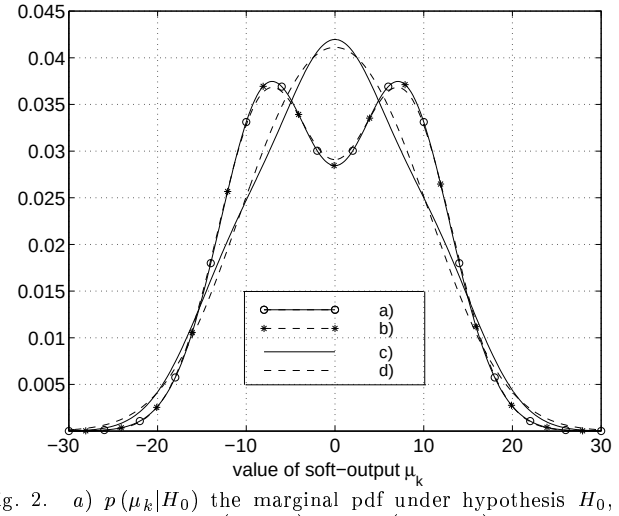

Fig. 2. *a)* $p(\mu_k|H_0)$ the marginal pdf under hypothesis H_0, *b)* Gaussian mixture $\frac{1}{2}\mathcal{N}\left(m_0,\sigma_0^2\right)+\frac{1}{2}\mathcal{N}\left(-m_0,\sigma_0^2\right)$, *c)* $p(\mu_k|H_1)$ the marginal pdf under hypothesis H_1, *d)* Gaussian mixture $\frac{1}{2}\mathcal{N}\left(m_1,\sigma_1^2\right)+\frac{1}{2}\mathcal{N}\left(-m_1,\sigma_1^2\right)$.

where the threshold η is suitably chosen to meet a desired probability of detection specification. Evaluating the joint pdf $p\left(\underline{\mu}_1^W|H_i\right)$ analytically has proven to be very difficult. For this reason, we investigate next several approximations that simplify the test in (7).

IV. Approximations Leading to Decision Rules

The following proposition motivates all the approximations in the section.

Proposition 1 *Under both hypotheses, the vector* $\underline{\mu}_i^W=[\mu_1,\cdots\mu_W]^T$, *where* μ_k *is given in* (6), *is zero-mean uncorrelated with a covariance matrix* $\frac{4}{\sigma^4}\left(1+\sigma^2\right)\mathbf{I}$.

Proof: First note that $\sum_{k=-\infty}^{\infty}\mathrm{sinc}^2\left(k-\epsilon^{(i)}\right)=1$, and $\sum_{m=-\infty}^{\infty}\mathrm{sinc}\left(m-\epsilon^{(i)}\right)\mathrm{sinc}\left(n-\epsilon^{(i)}\right)=0$ for $m\neq n$. Also note that $\{a_k\}$ and $\{\nu_k\}$ are both i.i.d. zero mean random sequences. From equation (6),

$$\begin{aligned}
&E[\mu_p\mu_q]=E[\nu_p\nu_q]\\
&+\frac{4}{\sigma^4}E\left[\sum_{m=-\infty}^{\infty}\sum_{n=-\infty}^{\infty}a_{p-m}a_{q-n}\mathrm{sinc}\left(m-\epsilon^{(i)}\right)\mathrm{sinc}\left(n-\epsilon^{(i)}\right)\right]\\
&=E[\nu_p\nu_q]+\frac{4}{\sigma^4}\sum_{m=-\infty}^{\infty}\mathrm{sinc}\left(m-\epsilon^{(i)}\right)\mathrm{sinc}\left(m-p+q-\epsilon^{(i)}\right)\\
&=\begin{cases}\frac{4}{\sigma^2}+\frac{4}{\sigma^4} & \text{if } p=q\\ 0 & \text{if } p\neq q\end{cases}. \qquad \square
\end{aligned}$$

Approximation 1 Proposition 1 states that μ_k are uncorrelated random variables. If we also make the assumption that they are *independent* (which is a stronger constraint than uncorrelated), we can substitute $p\left(\underline{\mu}_1^W|H_i\right)$ with the product of marginals $\prod_{k=1}^{W}p(\mu_k|H_i)$. The marginals $p(\mu_k|H_i)$ for $\epsilon^{(0)}=\frac{1}{4}$ and $\epsilon^{(1)}=\frac{1}{2}$ are depicted in Fig. 2 (Appendix A shows how the marginal is computed). Under this approximation, the decision rule becomes

$$\prod_{k=1}^{W}\frac{p(\mu_k|H_0)}{p(\mu_k|H_1)}\underset{H_1}{\overset{H_0}{\gtrless}}\eta. \tag{8}$$

Approximation 2 We further approximate each marginal $p(\mu_k|H_i)$ by a mixture of Gaussians $\frac{1}{2}\mathcal{N}\left(m_i,\sigma_i^2\right)+\frac{1}{2}\mathcal{N}\left(-m_i,\sigma_i^2\right)$ (Appendix A shows how to determine the parameters of the Gaussian mixtures). The approximation is a result of treating the sum of all ISI terms and the noise term in (22) collectively as a single zero-mean Gaussion random variable, with variance σ_i^2 as given in the Appendix. The goodness of this approximation is depicted in Fig. 2, where the true marginals are compared to the approximate pdfs. The decision rule (8) now becomes

$$\prod_{k=1}^{W}\frac{\left(2\sqrt{2\pi\sigma_0^2}\right)^{-1}\left(\mathrm{e}^{-\frac{(\mu_k-m_0)^2}{2\sigma_0^2}}+\mathrm{e}^{-\frac{(\mu_k+m_0)^2}{2\sigma_0^2}}\right)}{\left(2\sqrt{2\pi\sigma_1^2}\right)^{-1}\left(\mathrm{e}^{-\frac{(\mu_k-m_1)^2}{2\sigma_1^2}}+\mathrm{e}^{-\frac{(\mu_k+m_1)^2}{2\sigma_1^2}}\right)}\underset{H_1}{\overset{H_0}{\gtrless}}\eta, \tag{9}$$

where $\sigma_0^2=\frac{4}{\sigma^4}\left(1+\sigma^2-\mathrm{sinc}^2\epsilon^{(0)}\right)$, $m_0=\frac{2}{\sigma^2}\mathrm{sinc}\,\epsilon^{(0)}$, $m_1=\frac{2}{\sigma^2}\mathrm{sinc}\,\epsilon^{(1)}$, and $\sigma_1^2=\frac{4}{\sigma^4}\left(1+\sigma^2-\mathrm{sinc}^2\epsilon^{(1)}\right)$.

Approximation 3 Since

$$\mathrm{e}^{-\frac{(|\mu_k|-m_i)^2}{2\sigma_i^2}}\leq\mathrm{e}^{-\frac{(\mu_k-m_i)^2}{2\sigma_i^2}}+\mathrm{e}^{-\frac{(\mu_k+m_i)^2}{2\sigma_i^2}}\leq 2\mathrm{e}^{-\frac{(|\mu_k|-m_i)^2}{2\sigma_i^2}}, \tag{10}$$

we use the approximation

$$\mathrm{e}^{-\frac{(\mu_k-m_i)^2}{2\sigma_i^2}}+\mathrm{e}^{-\frac{(\mu_k+m_i)^2}{2\sigma_i^2}}\approx K\cdot\mathrm{e}^{-\frac{(|\mu_k|-m_i)^2}{2\sigma_i^2}}, \tag{11}$$

where K is a constant whose value is between 1 and 2. Substituting (11) into (9), taking the logarithm, and rearranging the equation, we get a new decision rule

$$\xi=\sum_{k=1}^{W}(|\mu_k|+C)^2\underset{H_0}{\overset{H_1}{\gtrless}}\tau, \tag{12}$$

where $C=\frac{m_0\sigma_1^2-m_1\sigma_0^2}{\sigma_0^2-\sigma_1^2}$ and τ is the new threshold.

In [17], the decision rule $\sum_{k=1}^{W}|\mu_k|\underset{<}{\overset{>}{}}\tau$ is used. We found that this rule, while acceptable as a first-order approximation, is suboptimal to the rule in (12). The decision rule in (12) has a constant C, which strikes a balance between the two hypotheses, and hence gives rise to a better performance when compared to the rule in [17].

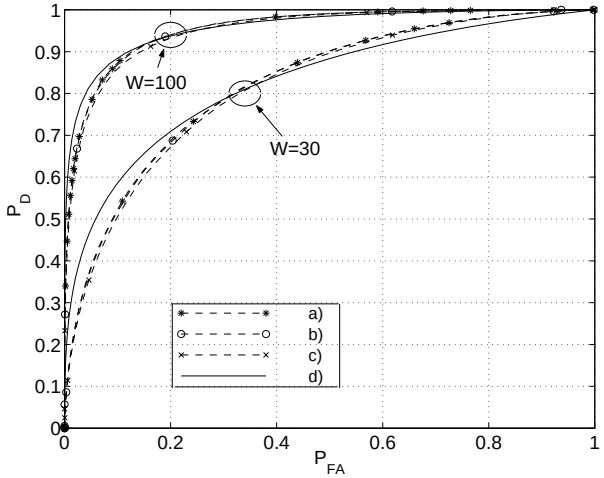

Fig. 3. ROC curves a) decision rule (8) in Approximation 1, b) decision rule (9) in Approximation 2, c) decision rule (12) in Approximation 3, d) formula (20) and (21) in Approximation 4.

Approximation 4 If we assume that μ_k are i.i.d., by the central limit theorem [16], for $W \to \infty$, ξ is a Gaussian random variable. Here we make a further assumption that ξ is Gaussian even when W is finite

$$(\xi|H_i) \sim \mathcal{N}\left(W \cdot m_{H_i}, W \cdot \sigma^2_{H_i}\right) \quad , \tag{13}$$

where

$$m_{H_i} = E\left[(|\mu_k| + C)^2 \,|H_i\right] \tag{14}$$

$$\sigma^2_{H_i} = Var\left[(|\mu_k| + C)^2 \,|H_i\right]. \tag{15}$$

Under both hypotheses, using Approximation 2, which assumes the pdf of μ_k is a mixture of Gaussians,

$$E\left[\,|\mu_k|\,|H_i\right] \cong \frac{2\sigma_i}{\sqrt{2\pi}} \mathrm{e}^{-\frac{m_i^2}{2\sigma_i^2}} + m_i \cdot \left[1 - \mathrm{erfc}\left(\frac{m_i}{\sqrt{2}\sigma_i}\right)\right] \tag{16}$$

$$E\left[\mu_k^2\,|H_i\right] \cong m_i^2 + \sigma_i^2 \tag{17}$$

$$E\left[\,|\mu_k|^3\,|H_i\right] \cong K_1 \cdot \mathrm{e}^{-\frac{m_i^2}{2\sigma_i^2}} + K_2 \cdot \left[1 - \mathrm{erfc}\left(\frac{m_i}{\sqrt{2}\sigma_i}\right)\right] \tag{18}$$

$$E\left[\mu_k^4\,|H_i\right] \cong m_i^4 + 6\sigma_i^2 m_i^2 + 3\sigma_i^4 \quad , \tag{19}$$

where $K_1 = \frac{2}{\sqrt{2\pi}}\left(m_i^2\sigma_i + 2\sigma_i^3\right)$, $K_2 = m_i^3 + 3m_i\sigma_i^2$, and $\mathrm{erfc}\,(x) = \frac{2}{\sqrt{\pi}} \int_x^\infty \mathrm{e}^{-t^2}\,\mathrm{d}t$.

We obtain the mean and variance of ξ under both hypotheses by substituting (16) – (19) into (14) and (15). If we then define the probability of detection P_D as the probability that H_1 is chosen when H_1 is true, and we define the probability of false alarm P_{FA} as the probability that H_1 is chosen when H_0 is true, we have the following analytic expressions

$$P_D\,(\tau, W) = \frac{1}{2}\mathrm{erfc}\left[\frac{\tau - W \cdot m_{H_1}}{\sqrt{2 \cdot W \cdot \sigma^2_{H_1}}}\right] \tag{20}$$

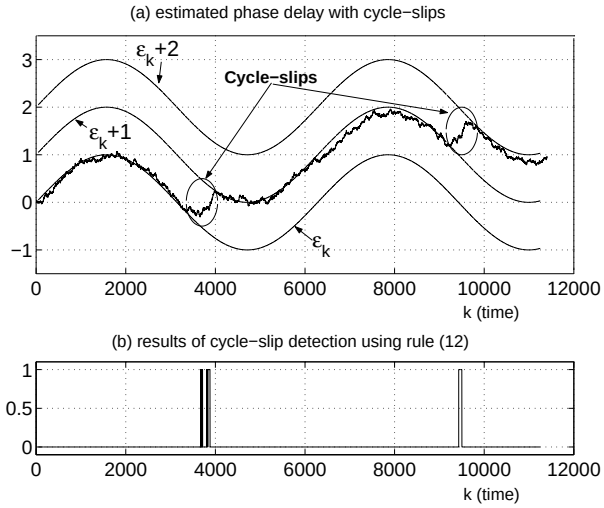

Fig. 4. (a) Estimated phase delay for a block containing two cycle-slips (b) Results of cycle-slip detection using rule (12). Multiple firings can be observed in one cycle-slip region, which means that the detector does not pinpoint the exact time instance of a cycle-slip (which is actually hard to define), but rather indicates a region (temporal window) where the cycle-slip occurs.

$$P_{FA}\,(\tau, W) = \frac{1}{2}\mathrm{erfc}\left[\frac{\tau - W \cdot m_{H_0}}{\sqrt{2 \cdot W \cdot \sigma^2_{H_0}}}\right] \quad , \tag{21}$$

where τ is the chosen threshold.

Comparison The receiver operating characteristic (ROC) curves (P_D vs. P_{FA}) for all decision rules are shown in Fig. 3. The curves corresponding to the decision rules in Approximations $1-3$ were obtained by Monte-Carlo simulations. The waveform samples were generated based on (6), where a_k is a sequence of i.i.d. binary random variables and μ_k is a white Gaussian random variable. The SNR is 6.0dB and W is the window size. We can see that the three ROC curves corresponding to decision rules in Approximations $1-3$ are very similar. The analytic result based on Approximation 4 has only a small difference from the first 3 curves (this difference falls to zero as $W \to \infty$). Approximation 4 is thus very useful for formulating a method for analytically determining the threshold τ and the window size W that will meet a desired specification of P_D and P_{FA}.

V. Application to Simulated Waveforms

Empirical evidence shows that for a Mueller and Müller synchronizer operating at SNR = 6dB, the system stays in the non-cycle-slip regime if $\epsilon \leq \epsilon^{(0)} = 0.2$. We set the desired P_D and P_{FA} to be 98% and 10%, respectively. For an SNR of 6dB, we find that the lowest window length satisfying (20) and (21) is $W = 116$ and the threshold is $\tau = 2990$. For these parameters we get $m_{H_0} = 23.93$, $m_{H_1} = 34.95$, $\sigma_{H_0} = 27.42$ and $\sigma_{H_1} = 39.21$. Fig. 4(a) gives the phase delay estimated by the Mueller and Müller

synchronizer with a first order loop filter [18] showing two cycle-slip regions. Fig. 4(b) shows the output of the cycle-slip detector using (12) as the decision rule (for SNR of 6dB, $C = -9.42$). The peaks in Fig. 4(b) correctly identify the regions of the two cycle slips. This example illustrates a general trend: at low SNRs, we need a long delay (large window size W) to detect cycle-slips.

VI. CONCLUSION

In this paper we have introduced a binary Bayesian cycle-slip detector that uses soft-output information to reach a decision. Using a series of approximations, we derived a practical decision rule. Simulation results showing ROC curves indicate that these approximations are reasonable. We also obtained analytic expressions for the probabilities of cycle-slip detection and false alarm that enable us to determine the window size and the threshold needed to meet a desired detector specification. An example has been shown that illustrates the applicability of the method on simulated waveforms. We generally conclude that a large delay (large window length) $W \geq 100$ samples is needed in order to detect cycle-slips with high reliability.

A. SOFT-OUTPUT INFORMATION STATISTICS

From (6), if we denote $\theta = \frac{2}{\sigma^2} \sum_{m=-\infty}^{\infty} a_{k-m} \mathrm{sinc}\left(m - \epsilon^{(i)}\right)$, we have $\mu_k = \theta + \nu_k$. Then the marginal pdf of μ_k under H_i is

$$p\left(\mu_k | H_i\right) = \int_{-\infty}^{\infty} \frac{1}{\sqrt{2\pi \frac{4}{\sigma^2}}} \mathrm{e}^{-\frac{(\mu_k - \theta)^2}{2\frac{4}{\sigma^2}}} p\left(\theta | H_i\right) \mathrm{d}\mu_k .$$

The pdf $p\left(\mu_k | H_i\right)$ is obtained by convolving the histogram of $(\theta | H_i)$ with a Gaussian pdf, to give a smooth curve depicted in Fig. 2. If we write (6) as

$$\mu_k = \frac{2a_k}{\sigma^2} \mathrm{sinc}\ \epsilon^{(i)} + \frac{2}{\sigma^2} \sum_{m \neq 0} a_{k-m} \mathrm{sinc}\left(m - \epsilon^{(i)}\right) + \nu_k, \quad (22)$$

It is easy to show that

$$\begin{aligned} m_i &= E\left[\mu_k | H_i, a_k = 1\right] = \frac{2}{\sigma^2} \mathrm{sinc}\ \epsilon^{(i)} \\ \sigma_i^2 &= \mathrm{Var}\left(\mu_k | H_i, a_k\right) = \frac{4}{\sigma^2}\left(1 + \sigma^2 - \mathrm{sinc}^2 \epsilon^{(i)}\right). \end{aligned}$$

References

[1] C. Berrou, A. Glavieux, and P. Thitimajshima, "Near Shannon limit error-correcting coding and decoding: Turbo-codes," in *Proc. IEEE Int. Conf. on Communications*, (Geneva, Switzerland), pp. 1064–1070, May 1993.

[2] R. G. Gallager, *Low-Density Parity-Check Codes*. Cambridge, MA: MIT Press, 1962.

[3] A. Richardson, T. Shokrollahi and R. Urbanke, "Design of provably good low-density parity check codes," *submitted to IEEE IT*, 1999.

[4] T. Richardson and R. Urbanke, "The capacity of low-density parity check codes under message-passing decoding," tech. rep., Bell-Labs, Lucent Technologies, Murray Hill, PA, 1999. submitted for publication in *IEEE Trans. Inform. Theory*; available at http://cm.bell-labs.com/who/tjr.

[5] M. G. Luby, M. Mitzenmacher, M. A. Shokrollahi, and D. A. Spielman, "Improved low density parity check codes using irregular graphs and belief propagation," in *Proc. IEEE Int. Symp. Inform. Theory*, (Cambrdge, MA), p. 117, Aug. 1998.

[6] D. J. C. MacKay, "Good error-correcting codes based on very sparce matrices," *IEEE Trans. Inform. Theory*, vol. 45, pp. 399–431, March 1999.

[7] J. Fan, A. Friedmann, E. Kurtas, and S. McLaughlin, "Low density parity check codes for partial response channels," *submitted for publication*, 2000.

[8] M. C. Reed and C. B. Schlegel, "An iterative receiver for partial response channels," in *Proc. IEEE Int. Symp. Inform. Theory*, (Cambrdge, MA), p. 63, Aug. 1998.

[9] W. Ryan, "Performance of high-rate turbo codes on PR4-equalized magnetic recording channels," in *Proc. IEEE Int. Conf. on Communications*, (Atlanta, GA), pp. 947–951, June 1998.

[10] J. Moon, Jan. 2000. Presentation at the NSIC quarterly review; sumbitted for publication.

[11] D. J. C. MacKay and M. C. Davey, "Evaluation of Gallager codes for short block length and high rate applications." available at http://www.keck.ucsf.edu/m̃ackay/, Jan. 1999.

[12] K. H. Mueller and M. Müller, "Timing recovery in digital synchronous data receivers," *IEEE Trans. Commun.*, vol. 24, pp. 516–531, May 1976.

[13] D. J. C. MacKay and R. M. Neal, "Near Shannon limit performance of low density parity check codes," *Electronics letters*, vol. 33, pp. 457–458, March 1997.

[14] C. N. Georghiades and D. L. Snyder, "The expectation-maximzation algorithm for symbol unsynchronized sequence detection," *IEEE Trans. Commun.*, vol. 39, pp. 54–61, Jan. 1991.

[15] H. Meyr, M. Moeneclaey, and S. A. Fechtel, *Digital Communication Receivers*. New York: John Wiley & Sons, Inc., 1997.

[16] J. G. Proakis, *Digital Communications*. New York: McGraw-Hill, 1997.

[17] B. Mielczarek and A. Svensson, "Post-decoding timing synchronization of turbo codes on AWGN channels," *Proceedings IEEE Vehicular Technology Conference*, pp. 1265–1270, May 2000.

[18] A. Patapoutian, "On phase-locked loop and Kalman filters," *IEEE Trans. Commun.*, vol. 47, pp. 670–672, May 1999.